Computer simulation study of a liquid crystal confined to a spherical cavity

Yu. Trukhina and T. Schilling
Institut für Physik, Johannes Gutenberg-Universität, Staudinger Weg 7, D-55099 Mainz, Germany
(Received 2 October 2007; published 7 January 2008)

The interplay of surface ordering and elasticity can be studied on the example of a liquid crystal confined to a cavity. We present a computer simulation study of a liquid of hard spherocylinders in a hard spherical cavity. With increasing density, first a uniaxial surface film forms and then a biaxial surface film, which eventually fills the entire cavity. We studied how the surface order, the adsorption, and the shape of the director field depend on the curvature of the wall. We find that orientational ordering at a curved wall is stronger than at a flat wall, while adsorption is weaker. For densities above the isotropic-nematic transition, we always find bipolar configurations.

DOI: 10.1103/PhysRevE.77.011701 PACS number(s): 64.70.M−, 61.20.Ja, 64.70.Ja

I. INTRODUCTION

Suspensions of anisotropic particles form a variety of phases that have both liquidlike and crystal-like properties. In particular, elongated particles undergo a phase transition from the isotropic phase, in which particle orientations and positions are disordered, to the nematic phase, in which orientations are aligned and positions are disordered. Materials made from elongated particles are of interest for technological applications, because the direction of preferred particle alignment (the director) can be easily manipulated and hence the optical properties of these materials can be tuned. This property has made liquid crystals the basis for a large range of technological devices [1].

When a liquid crystal is confined to a cavity, its director field becomes subject to competing forces: on the one hand, the surface of the cavity orients the director field ("surface anchoring"); on the other hand, deformations of the director field cost elastic energy. Hence the equilibrium director field is determined by a compromise between surface anchoring and elasticity. One example of a confined liquid crystal that has attracted particular interest from theoretical physicists is the nematic droplet. A nematic droplet inside a liquid environment (e.g., the coexisting isotropic phase or a polymer matrix) can adapt not only its director field but also its shape. Various authors have discussed the morphologies of nematic droplets in the framework of Frank elastic theory and Landau–de Gennes theory [2–5]. In particular, Prinsen and van der Schoot have recently given a detailed analysis of this problem [6–8].

Inspired by the development of polymer-dispersed liquid crystal displays, the properties of nematic droplets have also been studied in experiments and simulations [9–11]. In particular, Zannoni and co-workers performed several computer simulation studies of the Lebwohl-Lasher model inside a spherical cavity [12–19]. In this model the positional degrees of freedom are discretized, while the orientations vary continuously. The results, which we show in Sec. III B, agree well with their results.

The bulk phase behavior of hard spherocylinders is well known [20–22]. Less is known, however, about the effect confinement has on this model. Hard spherocylinders in contact with a planar hard wall have been studied within the Onsager approximation, i.e., for infinite aspect ratio, by Poniewierski and Hołyst [23,24]. They found that the wall induces parallel alignment and that the nematic phase wets the wall at isotropic-nematic (IN) coexistence. For spherocylinders of finite length, Dijkstra, van Roij, and Evans performed computer simulations [25] and calculations within the Zwanzig model [26]. They observed that an isotropic fluid brought into contact with a wall forms a uniaxial surface phase at low densities. At increasing density it undergoes a transition to a biaxial surface phase and finally, when the system approaches the IN transition, the wall is completely wet by a nematic film. We will refer to their work in more detail in Sec. III A. Groh and Dietrich studied the isotropic fluid of hard rods close to several curved wall geometries within the Onsager second virial approximation [27]. In particular, they found that the parallel alignment favored by the surface is stronger if the wall curves toward the fluid than if it curves away from it. In Sec. III A we compare these findings to our simulation results.

In this paper we present a computer simulation study of the phenomena that are caused by the interplay of surface anchoring and elasticity. In contrast to previous simulational work on this problem, we use a continuum model. In Sec. II we introduce the model and order parameters; Sec. III A contains results for concentrations in the bulk isotropic regime, and Sec. III B for the bulk nematic regime; and in Sec. IV we summarize.

II. MODEL AND OBSERVABLES

In the 1940s Onsager showed that the transition between the isotropic phase and the nematic phase is of entropic nature and that it can be explained by a simple geometrical argument [28]. Similarly to Onsager's approach, we consider hard spherocylinders each consisting of a cylinder of length L and diameter D capped by two hemispheres of diameter D. The location of the ith spherocylinder is given by its center of mass vector $\vec{r}_i$ and the orientational unit vector $\vec{u}_i$ pointing along the long axis of the particle (Fig. 1). We denote the distance from the particle to the center of the box as $r \equiv |\vec{r}|$. The particles are confined to a spherical cavity of radius R. The interaction between a particle and the wall of the cavity is hard.

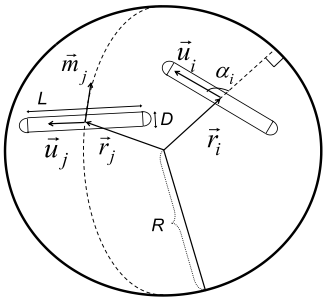

FIG. 1. Sketch to introduce definitions. The particles are confined in a spherical cavity of radius R. Each particle is a spherocylinder of length L and diameter D. The location of the ith spherocylinder is given by its center of mass vector $\vec{r}_i$ and the orientational unit vector $\vec{u}_i$. We denote the distance from the particle to the center of the box as $r \equiv |\vec{r}|$. $\vec{m}_i$ is the local meridian that lies on the plane defined by the z axis and the radial vector $\vec{r}_i$ of the particle. α is the angle between the orientational vector of the particle $\vec{u}_i$, and the normal to the surface $\vec{n}_i$ drawn from the center of the particle.

There are two main types of observables in this system: the density and the orientational order parameters.

We denote the density as the dimensionless quantity $\rho = (L+D)^2 DN/V$, where N is the number of particles and V is the volume of the system. The density in the middle of the box is denoted as ρ_b. As a reference we often use ρ_i, the density of the isotropic phase in coexistence with the nematic phase in the bulk.

The average alignment is defined in terms of the orientational traceless tensor $\mathbf{Q}$ with the elements

$$Q_{\alpha\beta} = \frac{1}{2N} \sum_{i=1}^{N} (3u_{i\alpha}u_{i\beta} - \delta_{\alpha\beta}),$$

where $u_{i\alpha}$ is the α component ($\alpha = x, y, z$) of the unit vector along the axis of particle i and $\delta_{\alpha\beta}$ is the Kronecker delta. Diagonalization of the tensor yields three eigenvalues λ_+, λ_0 and λ_-, where $\lambda_+ > \lambda_0 > \lambda_-$. The case $\lambda_+ > 0$, $\lambda_0 = \lambda_-$ corresponds to a structure with one preferred direction. The case $\lambda_+ = \lambda_0 > 0$ corresponds to a structure in which one direction is avoided and the two other directions are equally favored. All the intermediate cases $\lambda_+ > 0$, $\lambda_+ > \lambda_0 > \lambda_-$ correspond to a biaxial structure, and in an isotropic phase one finds $\lambda_+ = \lambda_0 = \lambda_- = 0$.

Various authors use different definitions of the nematic and biaxial order parameters [25,29]. To avoid confusion about the nematic order parameter, we plot the relevant eigenvalues instead. To detect biaxial order, we use $\Delta = \lambda_+ - \lambda_0$.

Depending on the structure there can be different types of symmetry in the system. For example, if we consider a simple case of a system in which there is no preferable orientation along any axis, there can be a tendency for the spherocylinders to orient parallel to the surface of the sphere. In this case there is radial symmetry. Therefore, one can calculate the orientational tensor directly by averaging over all configurations obtained in the simulations.

However, one has to proceed differently if there is an axis in the system along which the particles tend to align. As rotations of the overall director do not cost energy, the orientation of this axis fluctuates strongly. In order to average some local properties of interest the configurations need to be rotated in such a way that the director always points in the same direction (this, however, adds up noise). In the following, we call this direction the z axis.

If there is a cylindrical symmetry around the z axis and a top-down symmetry with respect to the x-y plane, then the particles can be interpreted as lying with their centers on a quarter of a circle with the coordinates $r_{xy} = \sqrt{r_x^2 + r_y^2}$ and $\varphi = \arcsin(|r_z| / \sqrt{r_x^2 + r_y^2})$.

In order to obtain spatially resolved information about the system, the simulation sphere is divided into bins of equal volume. We denote the number of particles in such a bin as $N(r_{xy}, \varphi)$. The orientational tensor $\mathbf{Q}$ is then accumulated in these bins over all the equilibrated conformations and only then are the eigenvalues calculated (and the biaxial order parameter accordingly). For the density the order of averaging does not change the result.

In order to describe the orientational order in the nematic phase we calculate the bipolar order parameter S_{bip}, which is defined as

$$S_{\text{bip}}(r_{xy}, \varphi) = \left\langle 1/N(r_{xy}, \varphi) \sum_{i=1}^{N(r_{xy},\varphi)} P_2(\vec{u}_i \cdot \vec{m}_i) \right\rangle,$$

where P_2 is the second-rank Legendre polynomial, $\vec{u}_i$ is the orientation vector of particle i, and $\vec{m}_i$ is the local meridian that lies on the plane defined by the z axis and the radial vector $\vec{r}_i$ of the particle (Fig. 1).

The alignment with respect to the z axis is characterized by

$$S_z(r_{xy}, \varphi) = \left\langle 1/N(r_{xy}, \varphi) \sum_{i=1}^{N(r_{xy},\varphi)} P_2(\vec{u}_i \cdot \vec{e}_z) \right\rangle,$$

where $\vec{e}_z$ is the unit vector pointing in the z direction.

III. RESULTS

A. The isotropic phase

We performed Monte Carlo simulations in the NVT ensemble. We considered spherocylinders of $L/D = 15$ confined to spherical cavities of radii R from $2.5L$ to $10L$. The number of particles was chosen such that we obtained an isotropic fluid in the center of the cavity. As a reference density we took the density of the isotropic phase at coexistence with the nematic phase in the bulk [25], $\rho_{\text{iso}} = 3.675$. The condition $\rho_b < 3.675$ corresponds to 400–50 000 particles depending on the size of the simulated system.

First, we consider how the structure of our system changes when the density is changed, while keeping the size of the confining sphere invariant ($R/L = 3.03$).

In Figs. 2 and 3 the equatorial profiles ($\sin\varphi = 0$) of the nematic and biaxial order parameters are shown for different values of the density ρ_b. One can see that in the system with the smallest density ($\rho_b = 2.13$, stars) the nematic order pa-

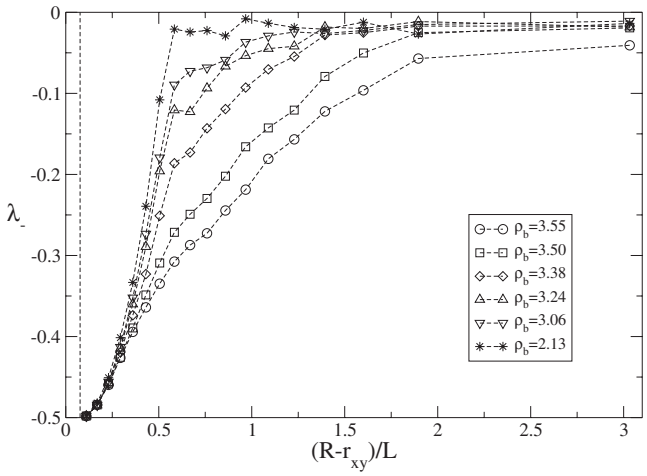

FIG. 2. Nematic order parameter versus distance from the wall for densities below the isotropic nematic transition. The vertical dashed line indicates the forbidden layer.

rameter λ_- is negative close to the wall and is approximately 0 far from it. The biaxial order parameter Δ is close to 0 everywhere. This means that the spherocylinders form an isotropic phase in the center of the sphere, while close to the wall there is a layer in which one direction is avoided (a "uniaxial surface phase"). With increasing density, Δ develops a maximum close to the wall, while it stays 0 in the center of the sphere. The peak gets wider and higher with increasing density. This indicates that the ordering of the spherocylinders becomes biaxial at the wall at higher densities.

We performed a set of additional runs to estimate the density at which the transition from the uniaxial to the biaxial surface phase occurs. $\Delta(r_{xy}=R)$ increases smoothly with density ρ_b (see Fig. 4). The transition happens at a density lying in the same range as predicted by theory [26] and estimated in a computer simulation for the same fluid of spherocylinders near a flat wall [25]. However, in the cavity

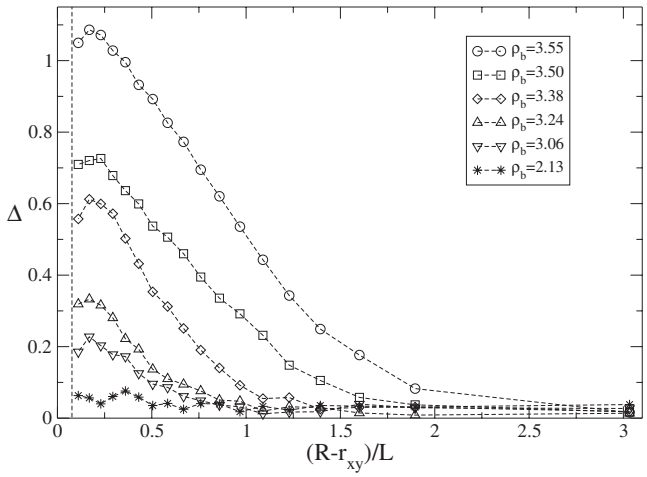

FIG. 3. Biaxial order parameter $\Delta=\lambda_+-\lambda_0$ versus distance from the wall for densities below the isotropic nematic transition. The vertical dashed line indicates the forbidden layer.

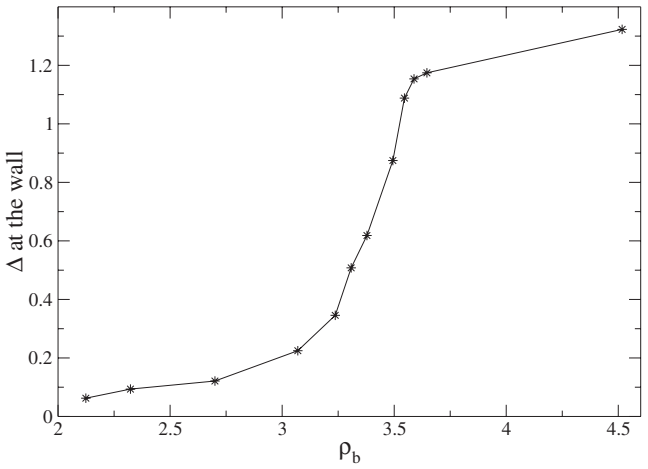

FIG. 4. Biaxiality at the wall versus density in the center of the sphere. There is a smooth transition from a uniaxial to a biaxial surface phase at $3 \leq \rho_b \leq 3.5$.

the transition becomes rounded because of finite system size.

In Figs. 2 and 3 one can see a dashed vertical line at $R - r_{xy} \approx 0.1L$. This line indicates a "forbidden" layer at the curved wall. This layer appears when the wall curves toward the elongated particles and they cannot approach it by their centers. We define the width of the forbidden layer as the distance between the wall and the center of a particle that touches the wall with both ends (Fig. 5). This forbidden layer can also be seen in Fig. 6, in which the profiles of the local density $\rho(r_{xy}, \sin\varphi=0)$ are shown for different values of the density ρ_b. All density profiles have a minimum close to the wall at $r_{xy}=R-\delta$. Further from the wall the density increases,

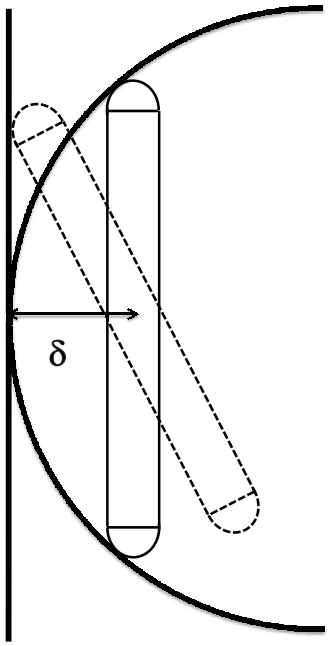

FIG. 5. Sketch of spherocylinders near a curved wall and a flat one: the dashed spherocylinder is allowed near the flat wall and is forbidden near the curved one. We define δ as the width of the forbidden layer near the curved wall.

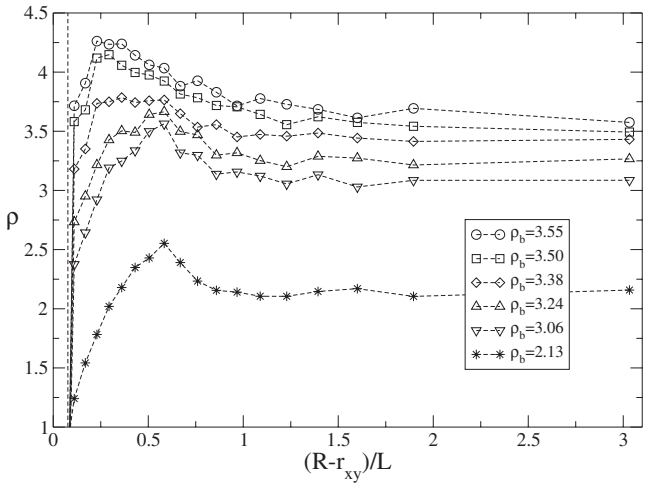

FIG. 6. Density versus distance from the wall for densities below the isotropic nematic transition. The vertical dashed line indicates the forbidden layer.

reaches its maximum, and then levels off into constant value ρ_b. For increasing density the cusp in the density profile moves closer to the wall. This effect can be explained by the profiles of the biaxial order parameter in Fig. 3, from which we can see that the value of Δ near the wall is increasing with increasing ρ_b, corresponding to a stronger biaxial ordering.

In Figs. 2 and 3 for small densities λ_- decays rapidly near the wall and slowly further from it. Two length scales seem to be involved. One is given by correlations with the wall orientation, the other by correlations between the particles.

Figure 7 shows the width of the oriented layer (measured as the width of the "inverted peaks" in λ_- at 1/2 of their depth) with respect to the reduced density $(\rho_i-\rho_b)/\rho_i$. The width of the layer increases roughly logarithmically as ρ_b approaches ρ_i. However, at the highest examined densities, the behavior changes, because, as one can see from Fig. 2, for these systems the fluid in the center of the sphere is not isotropic but has some preferred orientation of the rods. This

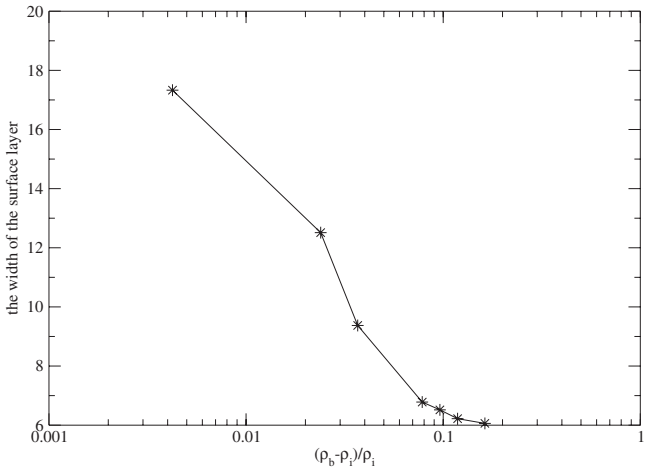

FIG. 7. Width of the surface layer in the profiles of λ_- versus reduced density $(\rho_i-\rho_b)/\rho_i$.

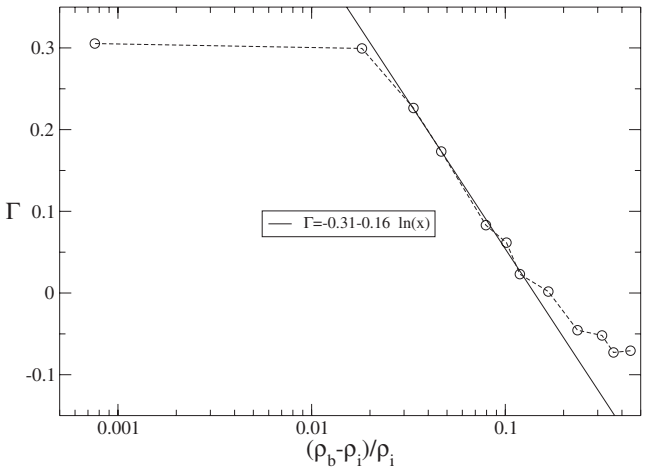

FIG. 8. Adsorption Γ versus $(\rho_i-\rho_b)/\rho_i$. For $0.01<(\rho_i-\rho_b)/\rho_i<0.11$ the adsorption depends logarithmically on $(\rho_i-\rho_b)/\rho_i$. For values closer to the bulk phase transition, the system becomes nematic. Hence the adsorption deviates from the logarithmic behavior. Fitting $\Gamma=a_0+a_1\ln[(\rho_i-\rho_b)/\rho_i]$ we find $a_0=-0.31$ and $a_1=-0.16$.

means that the biaxial layer expands to the whole cavity.

The ordering induced by the wall shows up not only in the orientational order, but also in the adsorption

$$\Gamma = \int [\rho(r_{xy}, \sin\phi = 0) - \rho_b] r_{xy}^2 dr_{xy}.$$

In Fig. 8 the adsorption Γ is shown versus $\ln(\rho_i-\rho_b)/\rho_i$. For $0.01<(\rho_i-\rho_b)/\rho_i<0.11$ the adsorption Γ depends logarithmically on $(\rho_i-\rho_b)/\rho_i$. For values closer to the bulk phase transition, the system becomes nematic. Hence the adsorption deviates from the logarithmic behavior. We fit $\Gamma=a_0+a_1\ln((\rho_i-\rho_b)/\rho_i)$ and find $a_0=-0.31$ and $a_1=-0.16$. Comparing to the values which were obtained for the Zwanzig model [26] ($a_1=-0.235$) and in the computer simulation of the same objects near a flat wall [25] ($a_1=-0.914$), we conclude that in the case of a curved wall the adsorption, i.e., density, grows less.

In order to describe orientational ordering with respect to the surface we introduce the parameter S_{surf} (note that the prefactor differs from the definitions of S_{bip} and S_z in order to facilitate comparison with the work by Groh and Dietrich [27])

$$S_{surf}(r_{xy}) = \langle 1/N(r_{xy}) \sum_{i=1}^{N(r_{xy})} \sqrt{5/(4\pi)} P_2(\vec{u}_i \cdot \vec{n}_i) \rangle$$

$$= \langle 1/N(r_{xy}) \sum_{i=1}^{N(r_{xy})} \sqrt{5/(16\pi)} (3\cos^2\alpha_i - 1) \rangle,$$

where α is the angle between the orientational vector of the particle $\vec{u}_i$ and the normal to the surface $\vec{n}_i$, drawn from the center of the particle (Fig. 1).

We show the profiles of this parameter in Fig. 9 for systems of $\rho_b=0.95$ and various radii. Close to the wall only the alignment parallel to the wall is allowed ($\alpha=\pi/2$); from this it follows that $S_{surf}(r_{xy}\to 0)=-\sqrt{5/(16\pi)}=-0.3154$. We can

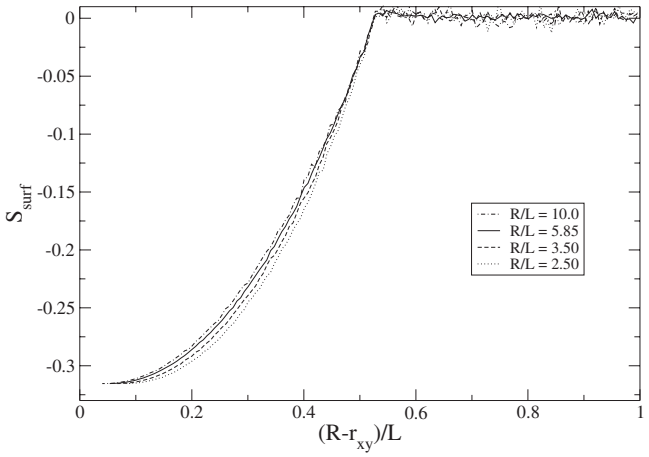

FIG. 9. Order parameter S_{surf} at a fixed density $\rho_b=0.95$ for different wall curvatures. Parallel orientations to the wall, i.e., negative values of S_{surf}, are more favored by strongly curved walls.

see this in the profiles for $r_{xy} \rightarrow (R-\delta)$. In the case of a random distribution one would get $S_{surf}^{iso}=0$. Negative values of S_{surf} indicate a preference of particles to lie parallel to the wall. S_{surf} is negative for distances from the wall that are less than $(L+D)/2$, and 0 further away. The alignment is stronger in the case of more strongly curved walls. This is explained by the fact that the curved wall restricts the possible orientations of the particles more strongly (see Fig. 5).

Summarizing, the wall induces an ordered layer. At low densities this layer is uniaxial; at higher densities it is biaxial (as it is in the case of a flat wall). Compared to the flat wall, however, orientational ordering is stronger, while adsorption is weaker. Hence the two main properties of the system that jump at the isotropic-nematic transition, density and orientational order, are influenced in opposite ways by a curved wall.

B. The nematic phase

Now we consider densities beyond the isotropic nematic transition. S_{bip} and S_z are shown in Figs. 10 and 11 for a system with $R/L=3.03$ and $\rho_b=4.55$. The density of the nematic phase at coexistence with the isotropic phase in the bulk [25] is $\rho_{nem}=4.3$. The S_{bip} parameter shows how close the configurations are to a bipolar one. The lines in Fig. 10 point in the direction of a perfectly bipolar field and their lengths correspond to the strength of alignment. Some small deviations can be seen at the poles of the sphere, while most of the field is bipolar. The S_z parameter measures the alignment of the director field with a homogeneous field. There are clear deviations. These findings are in agreement with the observations of Zannoni and co-workers [12,13].

We have varied the size of the system and its density for rods of lengths $L=7$ and 15. In all cases we found only the bipolar structure. Comparing to the arguments by Prinsen and van der Schoot [6] this implies that the energetic contribution from elastic deformations of the nematic director field is smaller than the contribution of the surface anchoring energy for all the examined system sizes and densities.

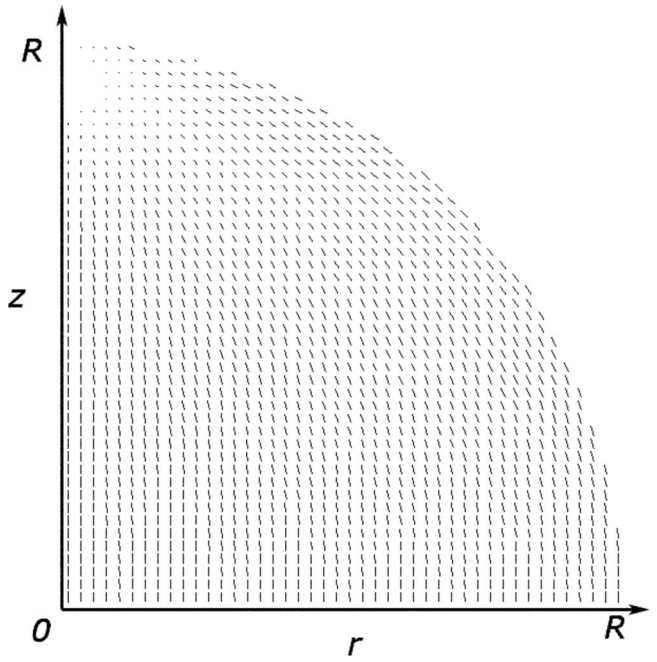

FIG. 10. Alignment with respect to an ideal bipolar structure: the lines point in the direction of the meridians; their length is given by the bipolar order parameter S_{bip}.

However, the structure that we obtain differs from the ideal bipolar one (see Fig. 10). This gives rise to the question: What properties does the defect on the poles have? Figure 12 shows the dependences of the eigenvalues of the orientational tensor **Q** of the particles lying on the z axis of the system (which is defined as the orientation of the overall nematic director field) on the distance from the pole of the

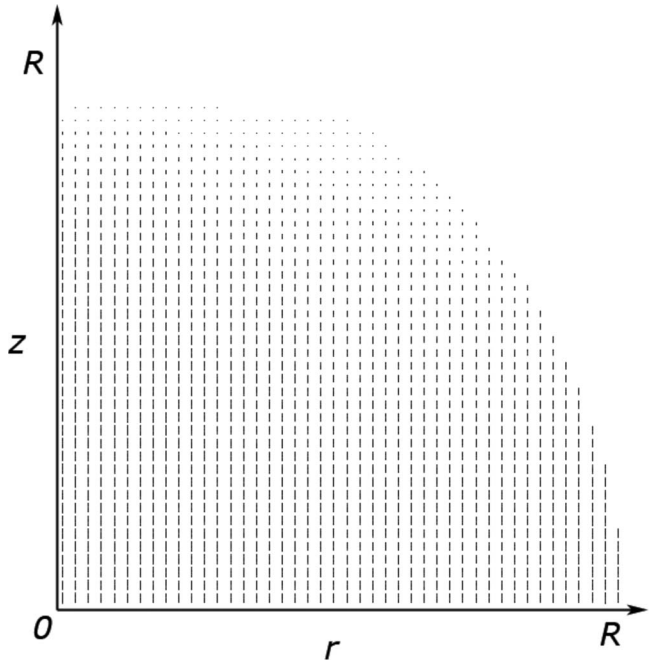

FIG. 11. Alignment with respect to an ideal homogeneous structure: the lines point in the z direction; their length is given by the parameter S_z.

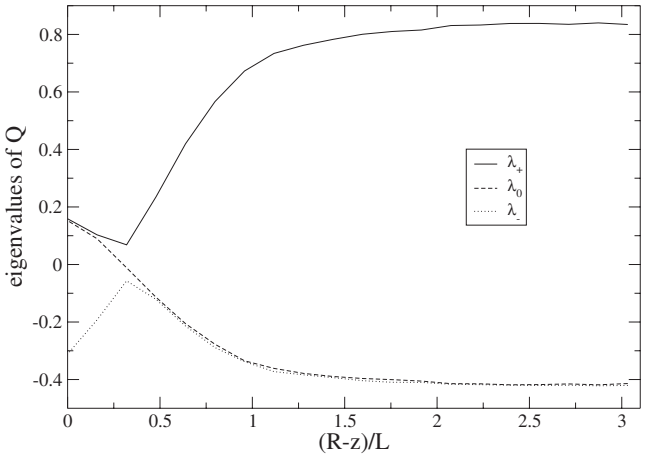

FIG. 12. Eigenvalues of the orientational tensor **Q** for the particles lying on the z axis of the system versus the distance from the pole of the sphere. The defect extends roughly $L/2$ into the sphere.

sphere. From the graph one can conclude that there is a highly ordered nematic phase in the center of the sphere. At a distance from the wall $z \sim L$, the nematic order parameter starts decaying until it reaches its minimum at $z \sim L/2$. At the same time one can see that at $z \sim L/2$ the difference between λ_- and λ_0 starts growing, indicating the presence of a biaxial structure. Directly at the wall ($z=0$), $\lambda_+ = \lambda_0$, while $\lambda_- = -0.3$; this means the system forms a uniaxial surface phase at the wall. (This behavior is independent of the radius R of the confining sphere.) At this point one has to take into account that the averaging was done assuming radial symmetry.

To get a better understanding of the structure of the defect we inspect snapshots of the system. A typical one is presented in Fig. 13, in which the droplet is seen from the top i.e., looking at one of the poles. We never observe an ideal bipolar configuration, which means that a boojum defect is energetically too expensive. Using this fact and taking into account the analysis of the values of the eigenvalues of the orientational tensor, we conclude that the point defect splits into a line of strength $k=1/2$ defects, which extends roughly to $r=L/2$ into the droplet. We could not investigate this in more detail because the averaging procedure needs to project conformations onto each other with respect to the nematic director of the entire droplet and the local director at the pole. As both quantities are subject to strong fluctuations, the quality of the averaged data is not high enough to allow for further conclusions.

IV. DISCUSSION AND SUMMARY

We have studied a fluid of hard spherocylinders with $L/D=15$ confined to a spherical cavity of $R/L=2.5,\ldots,10$. We have performed simulations for different values of the system density. At low values of the density we have observed an isotropic phase in the middle of the cavity and a layer of particles lying parallel to the wall at the surface. The curved wall favors parallel alignment. When the density of the system is increased the oriented layer grows. As predicted by Groh and Dietrich [27], a curved wall produces stronger parallel anchoring than a flat wall.

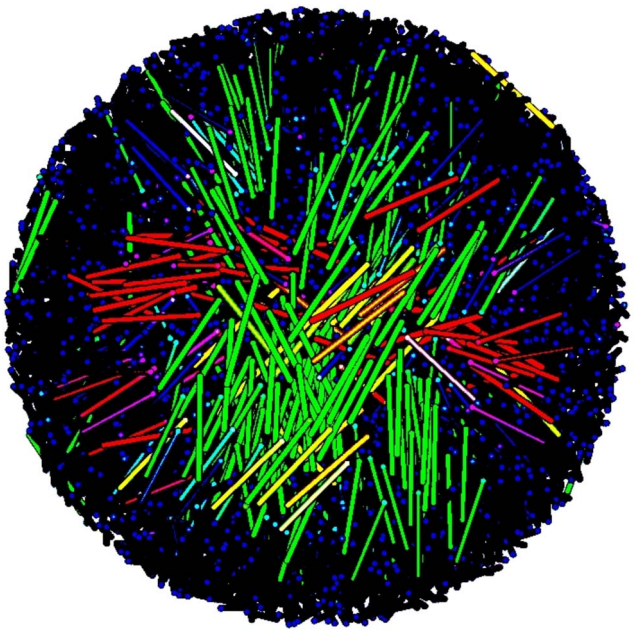

FIG. 13. (Color online) Typical snapshot of a pole of the sphere. The particles are coded by gray scale (color) according to their orientations.

Also, at low densities we have observed a rounded surface transition from a uniaxial to a biaxial phase. The thickness of the biaxial (nematic) layer at the surface increases logarithmically with the density until the entire cavity is filled with a nematic phase.

We also computed the adsorption at the wall. While orientational ordering is favored by the curved wall, adsorption is disfavored, compared to the case of a flat wall.

Simulations at higher densities (beyond the bulk nematic coexistence density in the center of the sphere) always produced bipolar droplets. This is consistent with theoretical predictions [6] if one assumes that for this model the energetic contribution due to the anchoring strength ω is always larger than the energetic contribution due to the elasticity.

The obtained bipolar structure differs from an ideal one in which the particles form boojums at the poles of the sphere. Apparently this type of defect is energetically too expensive. The point defect probably splits into a line of $k=1/2$ defects which extends roughly to $r=L/2$ into the droplet.

ACKNOWLEDGMENTS

We thank K. Binder, P. van der Schoot, and M. Allen for helpful suggestions. CPU time was provided on the JUMP by the John von Neumann Centre in Jülich. We thank the Deutsche Forschungsgemeinschaft (DFG, Emmy Noether Program) and the MWFZ Mainz for financial support.

[1] P. G. de Gennes and J. Prost, *The Physics of Liquid Crystals* (Clarendon Press, Oxford, 1993).
[2] S. Chandrasekhar, Mol. Cryst. **2**, 71 (1966).
[3] E. Dubois-Violette and O. Parodi, J. Phys. (Paris) Colloq. **30**, C4 57 (1969).
[4] R. D. Williams, J. Phys. A **19**, 3211 (1986).
[5] W. Huang and G. F. Tuthill, Phys. Rev. E **49**, 570 (1994).
[6] P. Prinsen and P. van der Schoot, Phys. Rev. E **68**, 021701 (2003).
[7] P. Prinsen and P. van der Schoot, Eur. Phys. J. E **13**, 35 (2004).
[8] P. Prinsen and P. van der Schoot, J. Phys.: Condens. Matter **16**, 8835 (2004).
[9] A. Golemme, S. Žumer, D. W. Allender, and J. W. Doane, Phys. Rev. Lett. **61**, 2937 (1988).
[10] J. H. Erdmann, S. Žumer, and J. W. Doane, Phys. Rev. Lett. **64**, 1907 (1990).
[11] O. O. Prishchepa, A. V. Shabanov, and V. Y. Zyryanov, Phys. Rev. E **72**, 031712 (2005).
[12] E. Berggren, C. Zannoni, C. Chiccoli, P. Pasini, and F. Semeria, Phys. Rev. E **50**, 2929 (1994).
[13] C. Chiccoli, Y. Lansac, P. Pasini, J. Stelzer, and C. Zannoni, Mol. Cryst. Liq. Cryst. Sci. Technol., Sect. A **372**, 157 (2001).
[14] C. Chiccoli, P. Pasini, I. Feruli, and C. Zannoni, Mol. Cryst. Liq. Cryst. **441**, 319 (2005).
[15] C. Chiccoli, P. Pasini, F. Semeria, and C. Zannoni, Phys. Lett. A **150**, 311 (1990).
[16] C. Chiccoli, P. Pasini, F. Semeria, and C. Zannoni, Mol. Cryst. Liq. Cryst. Sci. Technol., Sect. A **221**, 19 (1992).
[17] C. Chiccoli, P. Pasini, F. Semeria, and C. Zannoni, Mol. Cryst. Liq. Cryst. Sci. Technol., Sect. A **212**, 197 (1992).
[18] F. S. C. Chiccoli, P. Pasini, T. J. Sluchin, and C. Zannoni, J. Phys. II **5**, 427 (1995).
[19] E. Berggren, C. Zannoni, C. Chiccoli, P. Pasini, and F. Semeria, Chem. Phys. Lett. **197**, 224 (1992).
[20] P. Bolhuis and D. Frenkel, J. Chem. Phys. **106**, 666 (1997).
[21] S. C. McGrother, D. C. Williamson, and G. Jackson, J. Chem. Phys. **104**, 6755 (1996).
[22] H. Graf and H. Löwen, J. Phys.: Condens. Matter **11**, 1435 (1999).
[23] A. Poniewierski and R. Hołyst, Phys. Rev. A **38**, 3721 (1988).
[24] A. Poniewierski, Phys. Rev. E **47**, 3396 (1993).
[25] M. Dijkstra, R. van Roij, and R. Evans, Phys. Rev. E **63**, 051703 (2001).
[26] R. van Roij, M. Dijkstra, and R. Evans, J. Chem. Phys. **113**, 7689 (2000).
[27] B. Groh and S. Dietrich, Phys. Rev. E **59**, 4216 (1999).
[28] L. Onsager, Ann. N. Y. Acad. Sci. **51**, 627 (1949).
[29] R. J. Low, Eur. J. Phys. **23**, 111 (2002).